Embry-Riddle Aeronautical University

Matthew Zettergren, Meghan Burleigh

Summary of modeling capabilities

Local ionospheric models *available* for RENU2

Name	Grid type	Mathematical model	Possible use
Gemini (M. Zettergren)	2D, dipole (90-3000 km alt.)	Fluid, Maxwellian distribution	F-region and near topside upflows and plasma structures
Gemini 3D (M. Zettergren)	3D, Cartesian (90-1000 km alt.)	Fluid, Maxwellian distribution	Plasma structures and low altitude upflow processes
Gemini-TIA (M. Burleigh)	2D, dipole (90-20000 km alt.)	Fluid, Bi-Maxwellian distribution	Frictional heating, transverse heating, and topside upflow/outflow

Gemini

Modeled MICA density cavities

- Each DC electric field intensification associated with density depletion
- Depletions intermittently observed during ISR experiment
- Associated with growth phase and N-S streamer-related electric fields.

- ***Careful model decomposition shows these are due to molecular ion generation and enhanced recombination***

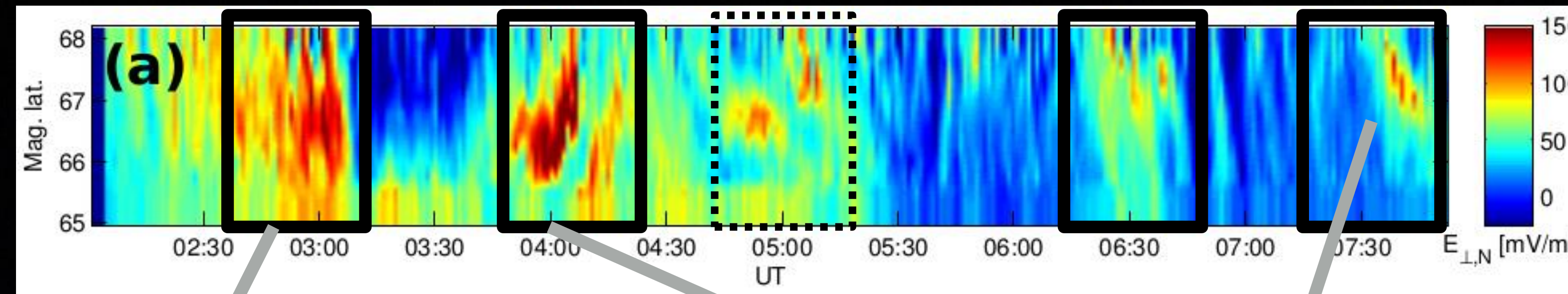

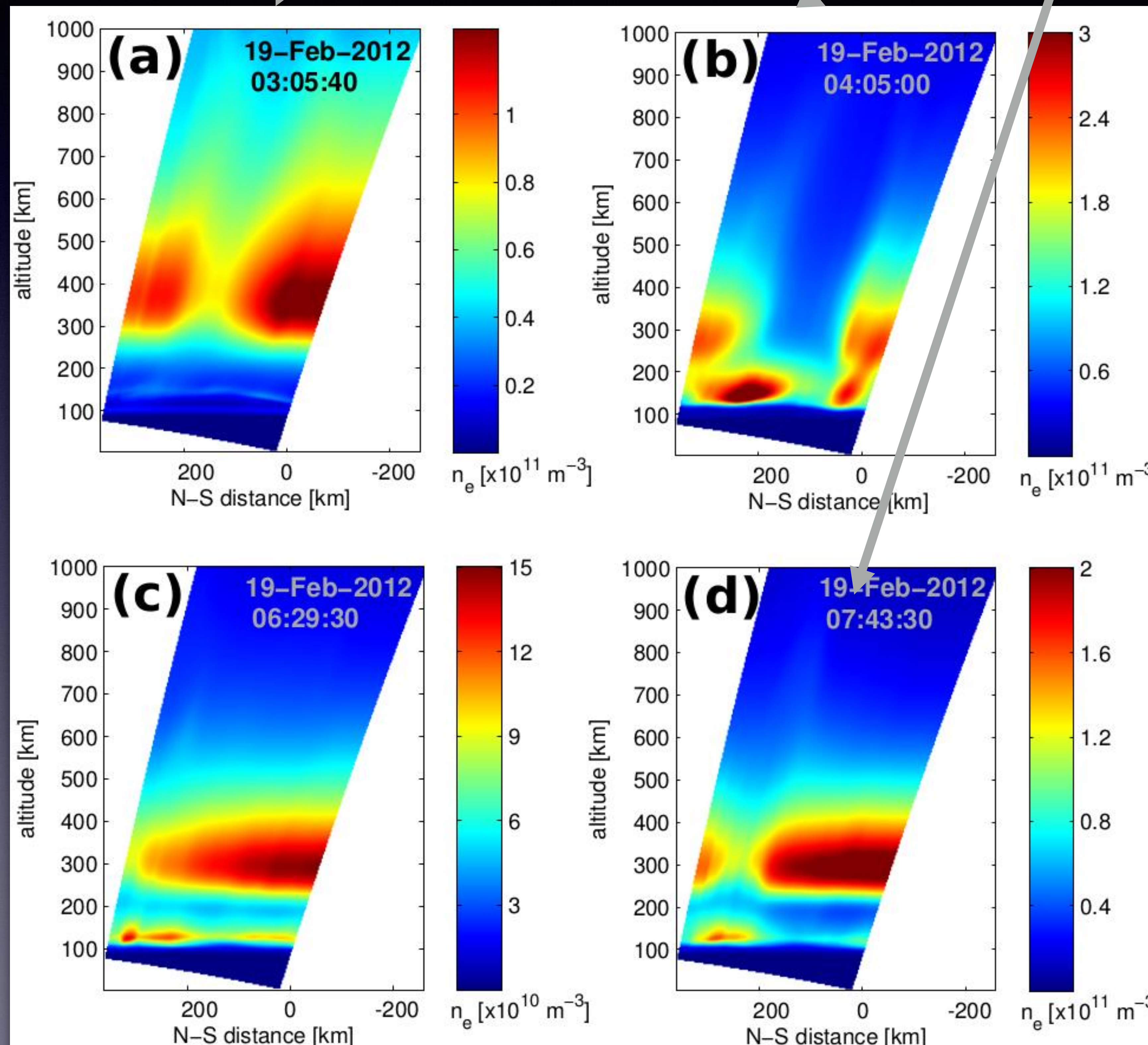

Fields and currents for fine-scale modeling

INPUT

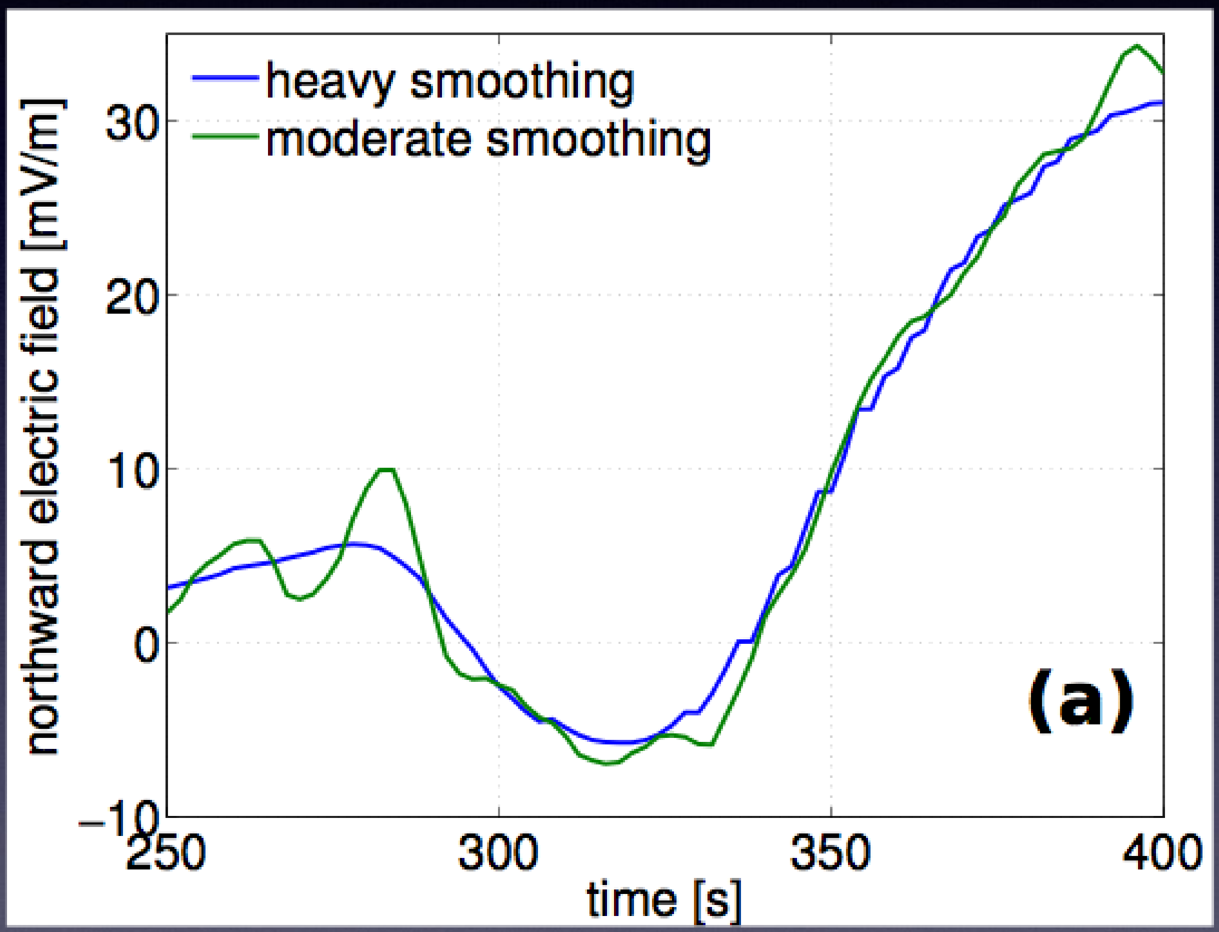

OUTPUT

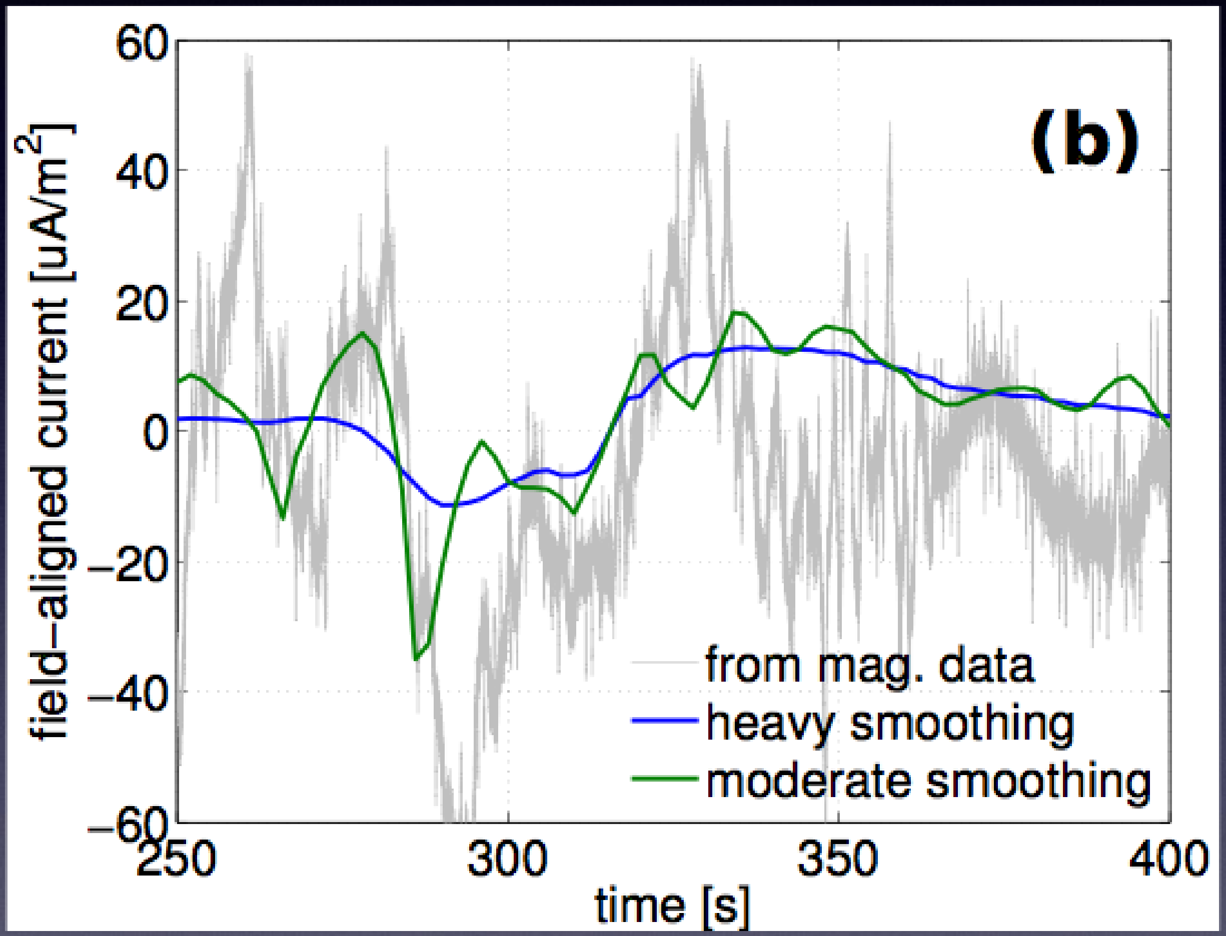

The model is able to mimic the basic electrostatic structure of the current systems

Contributions to total current density

Heavily smoothed simulation

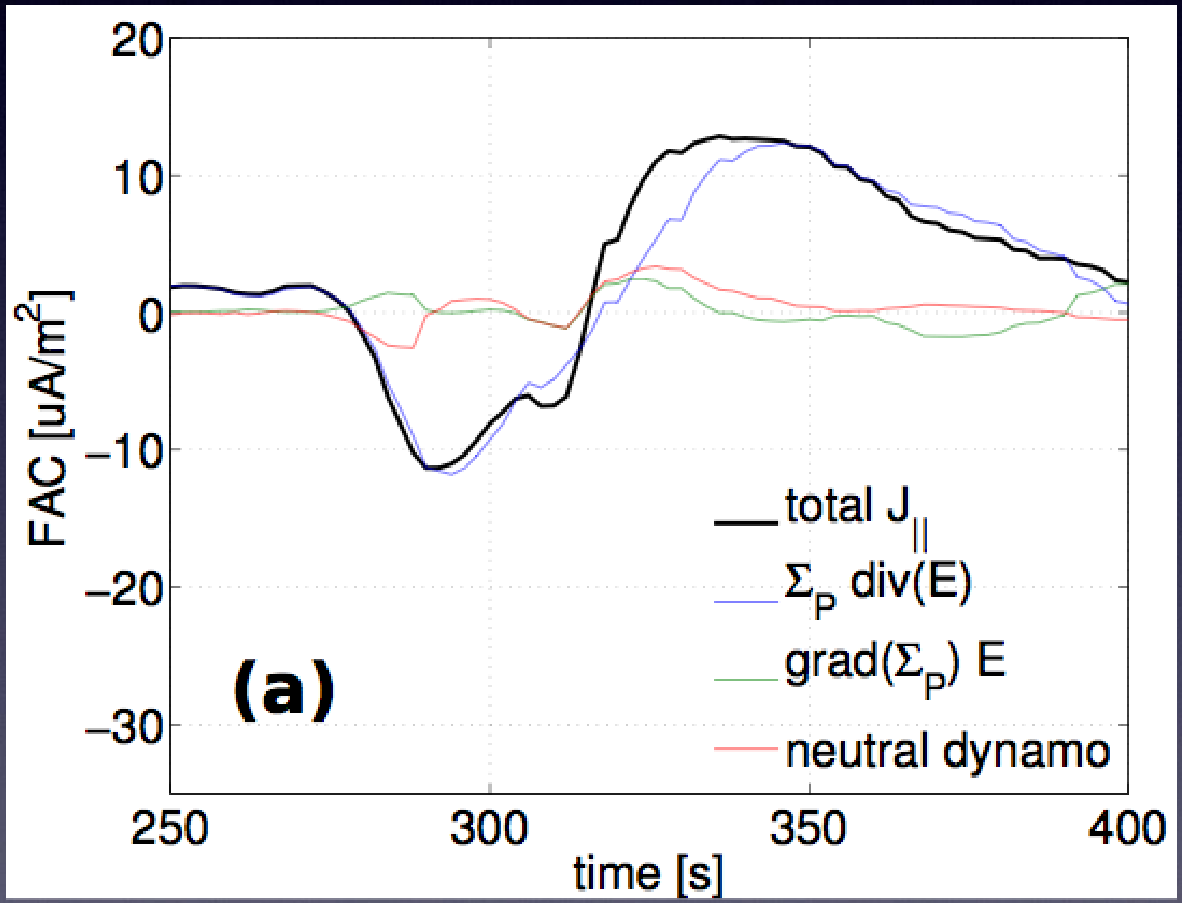

Moderately smoothed simulation

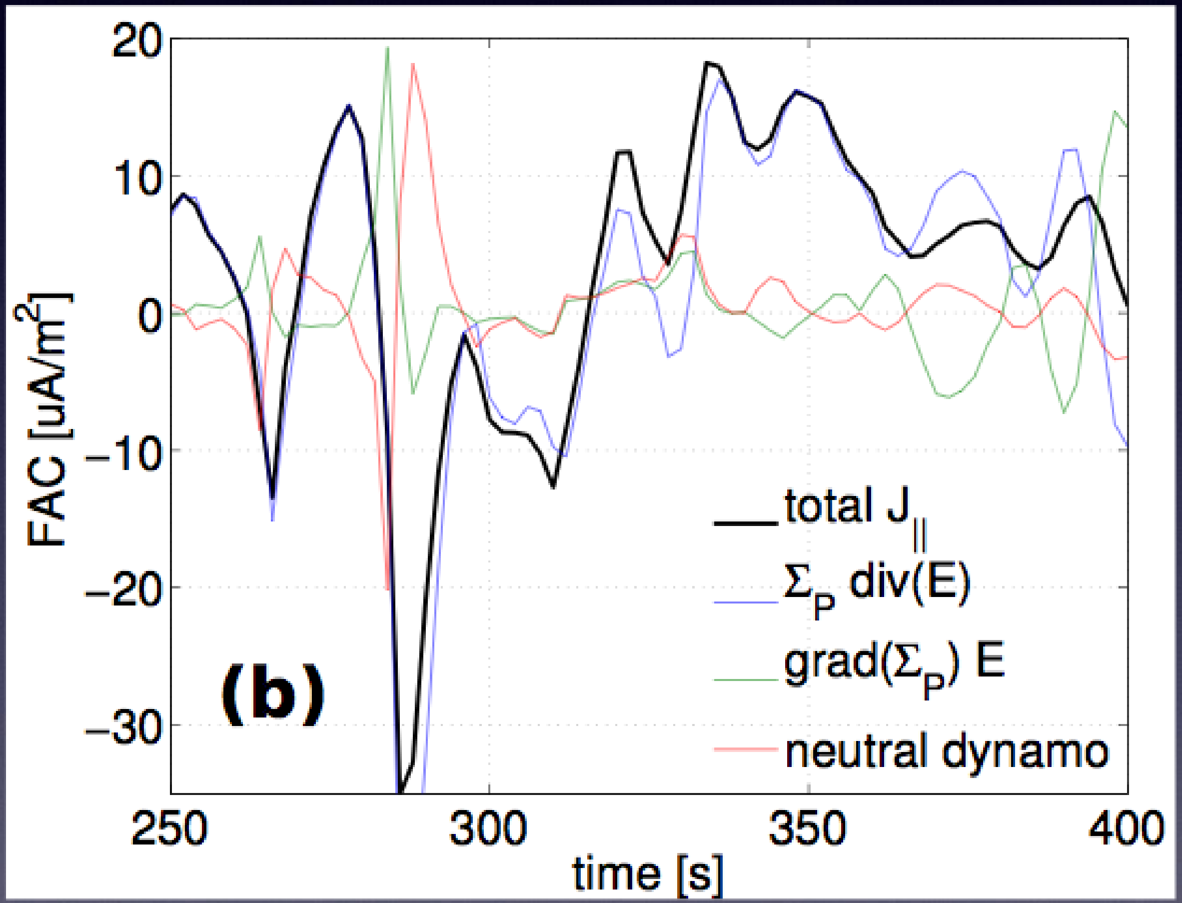

Electric field divergence dominates FAC, except near the up-to-down transition where conductivity gradients and winds contribute

Gemini 3D

Used to study gradient-drift instability effects on plasma density cavities [Zettergren, et al 2015b]

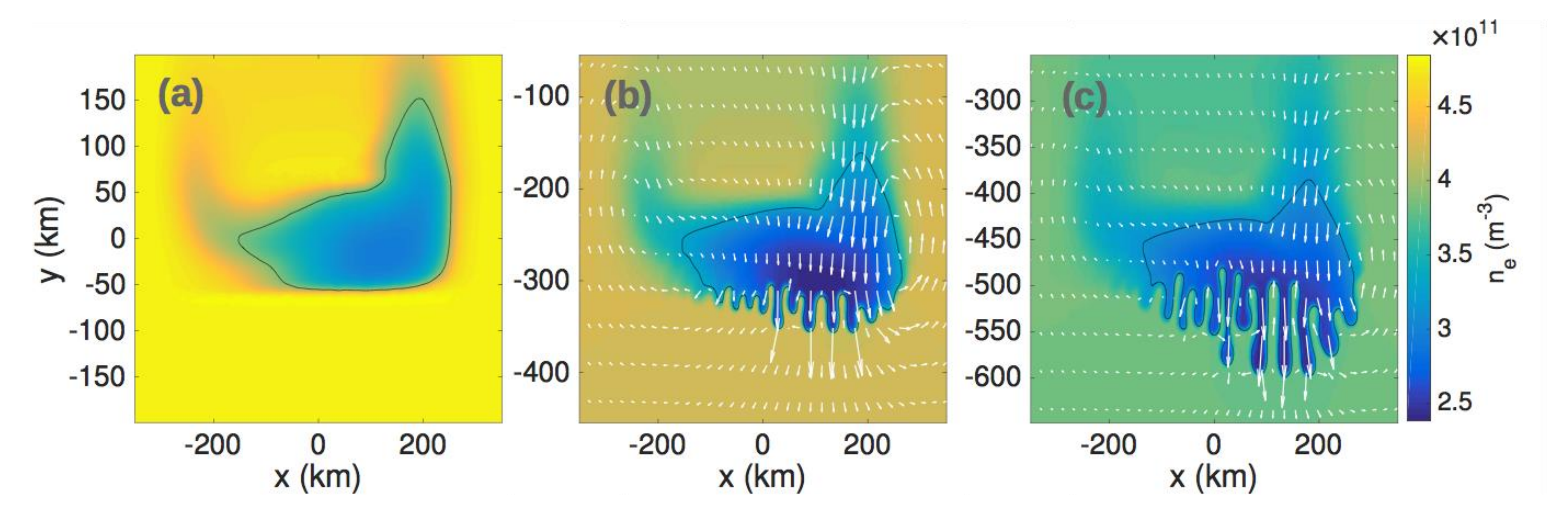

Gemini-TIA

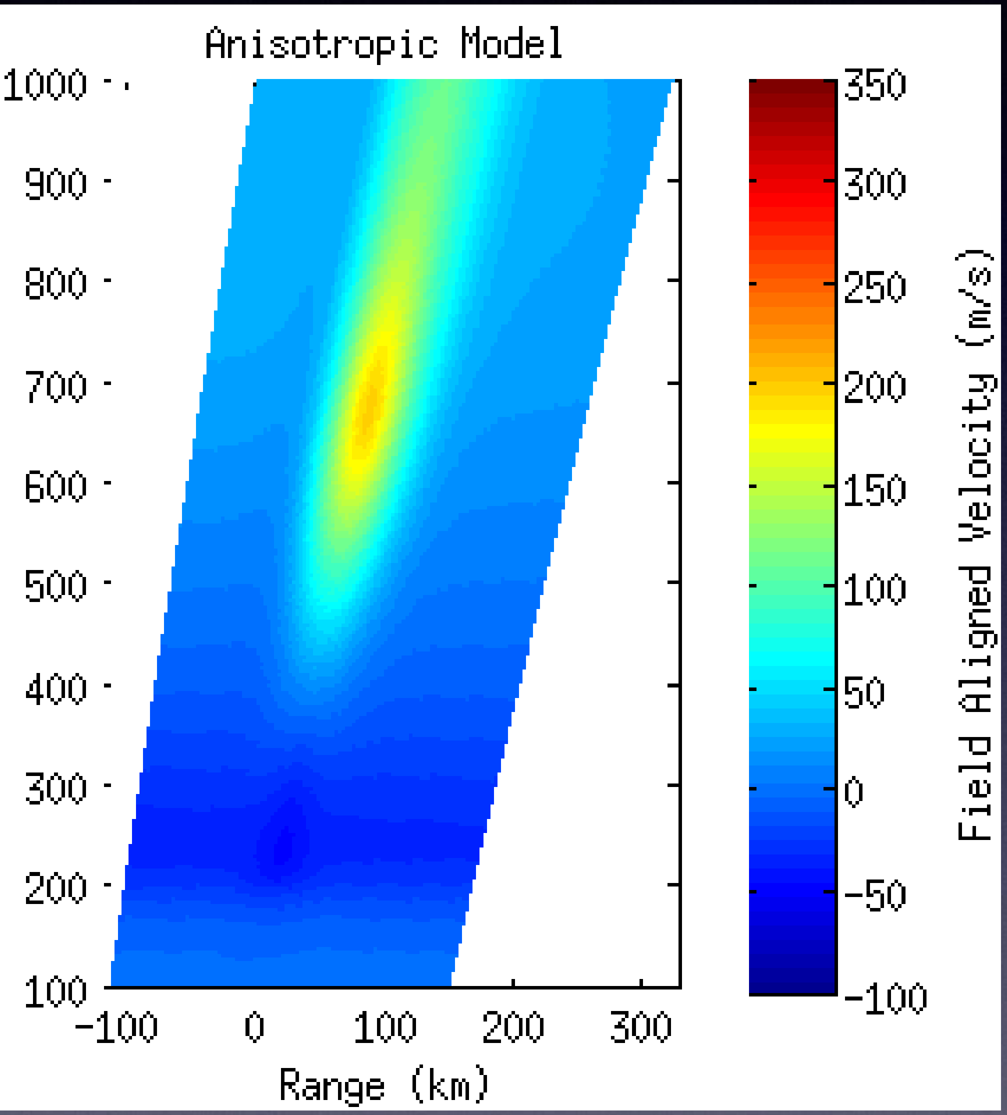

This model has been used to look at how the effects of properly including anisotropy impacts simulated ion upflows as well as the thermospheric modulation of ion upflows.

- Self consistently solves the time-dependent, nonlinear equations of conservation of mass, momentum, parallel energy, and perpendicular energy
- Seven ion species important to the E-, F-, and topside ionospheric regions: O^{+}, NO^{+}, N_2^{+}, O_2^{+}, N^{+}, H^{+}, and e^{-}
- Functions at altitudes from the lower E-region all the way up to several Earth radii
- Chemical and collisional interactions: ion-ion and ion-neutral
- Effects of photoionization and electron impact ionization.

RENU2 (Gemini-TIA)

13 December 2015 at 7:34 UTC

Data Inputs

- Trajectory
- Processed optical data
- Electron precipitation - vs. t
- DC Electric fields - vs. t
- BBELF PSD at oxygen gyro frequency - vs. t
- Neutral temperature and density – vs. t

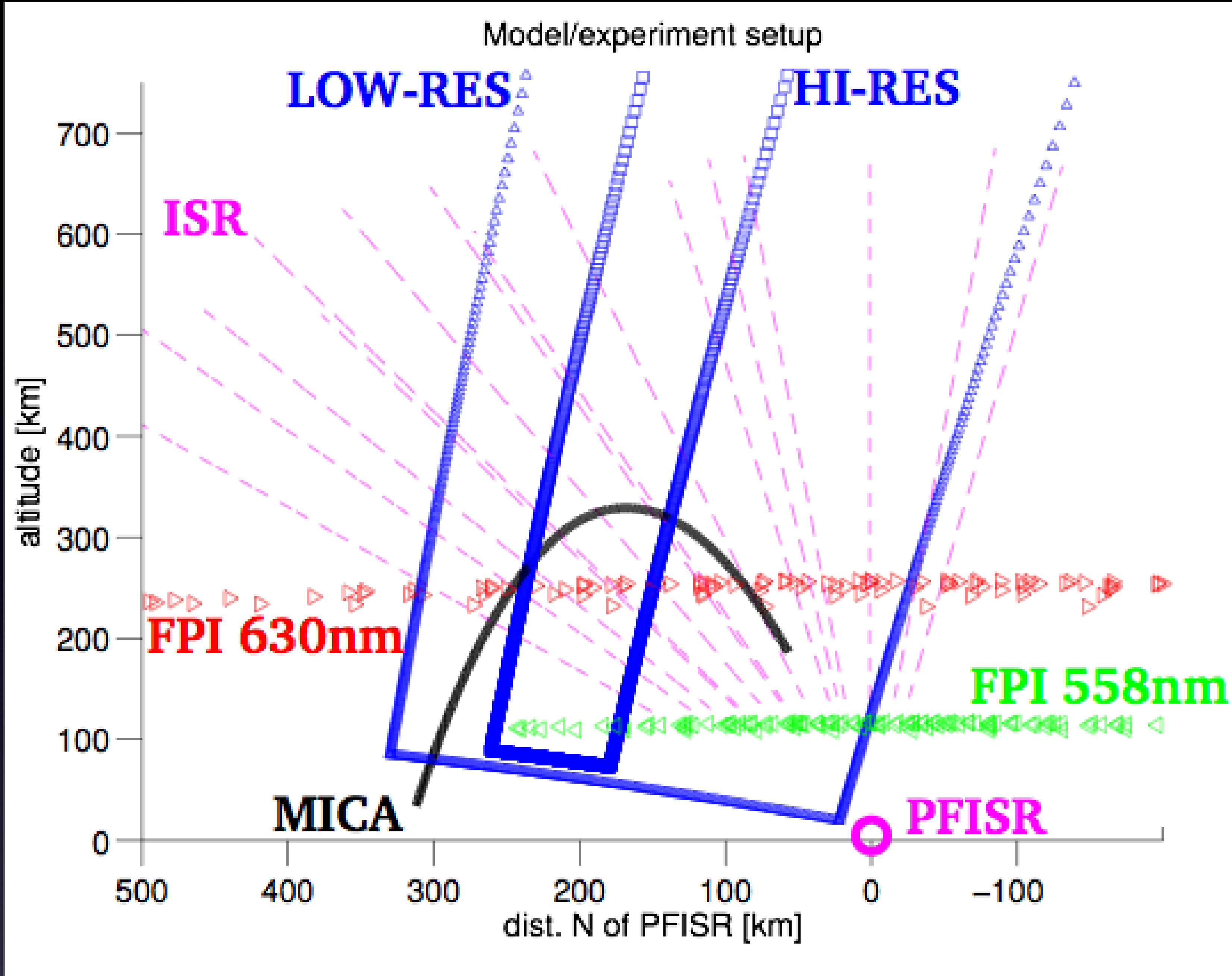

Moving beyond simple descriptions of upflow *drivers*

MICA example:

- ISR flows/fields via [Heinselman and Nicholls, 2008]
- SDI (FPI) winds [Conde et al]
- SDI + filtered allsky imager yields precipitation [D. Hampton]

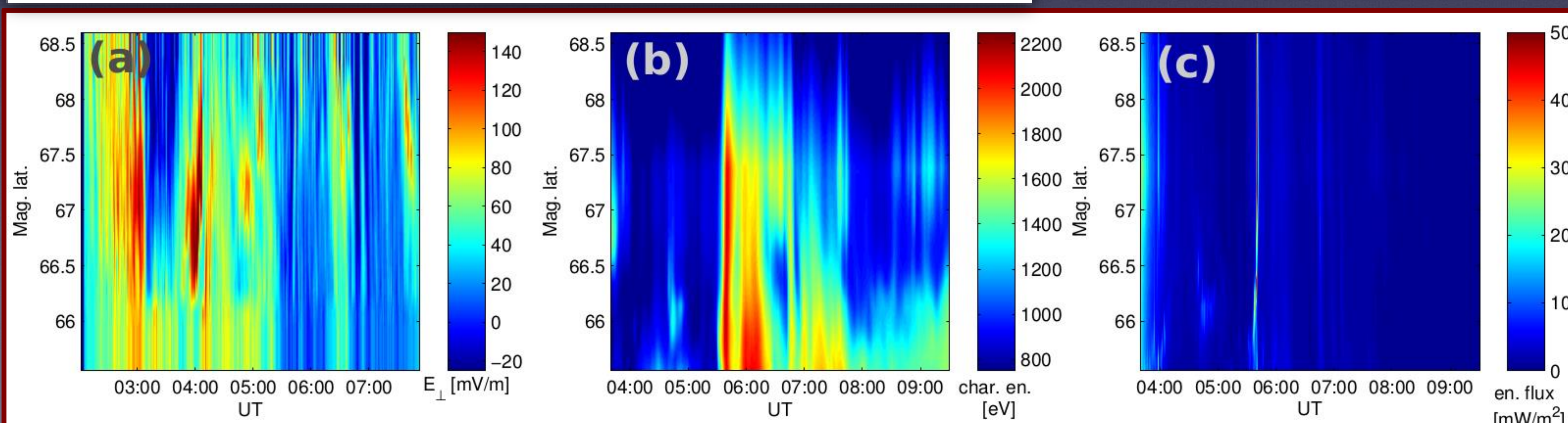

Data driven ion upflow:

- Upflow types: Type-1, type-2, neutral winds, wave-particle interactions, etc.
- Ion and electron responses to time dependent inputs
- Decompose resulting ion upflow to determine primary driver(s) if many are included
- Analyze FAC contributions
- See how the model's N_2^+ responses compare to the Aerospace PMT data

Backup Slides

MICA (Gemini)

19 February 2012 at 5:41:06.745 UT

Zettergren, et al 2014; Lynch, et al 2015; Fernandes, et al 2016

MICA rocket campaign: ISR density depletions

- MICA experiment 2-8 UT, 19 Feb. 2012
- Rocket launch at ~5:41 UT
- Density depletions fairly well correlated with ion temperature enhancements
- This matches theoretical expectations for conversion to molecular ions and subsequent recombination in a DCR

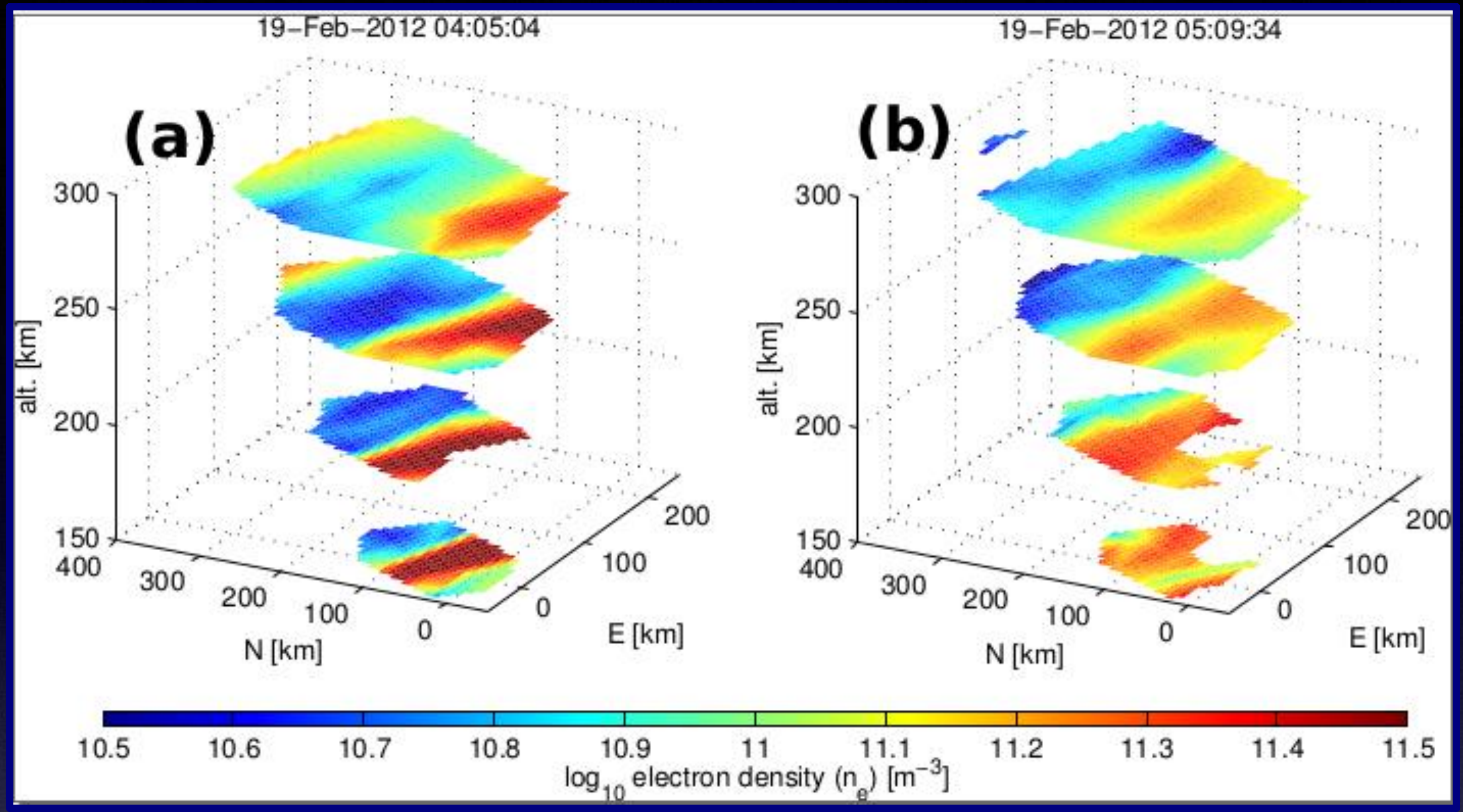

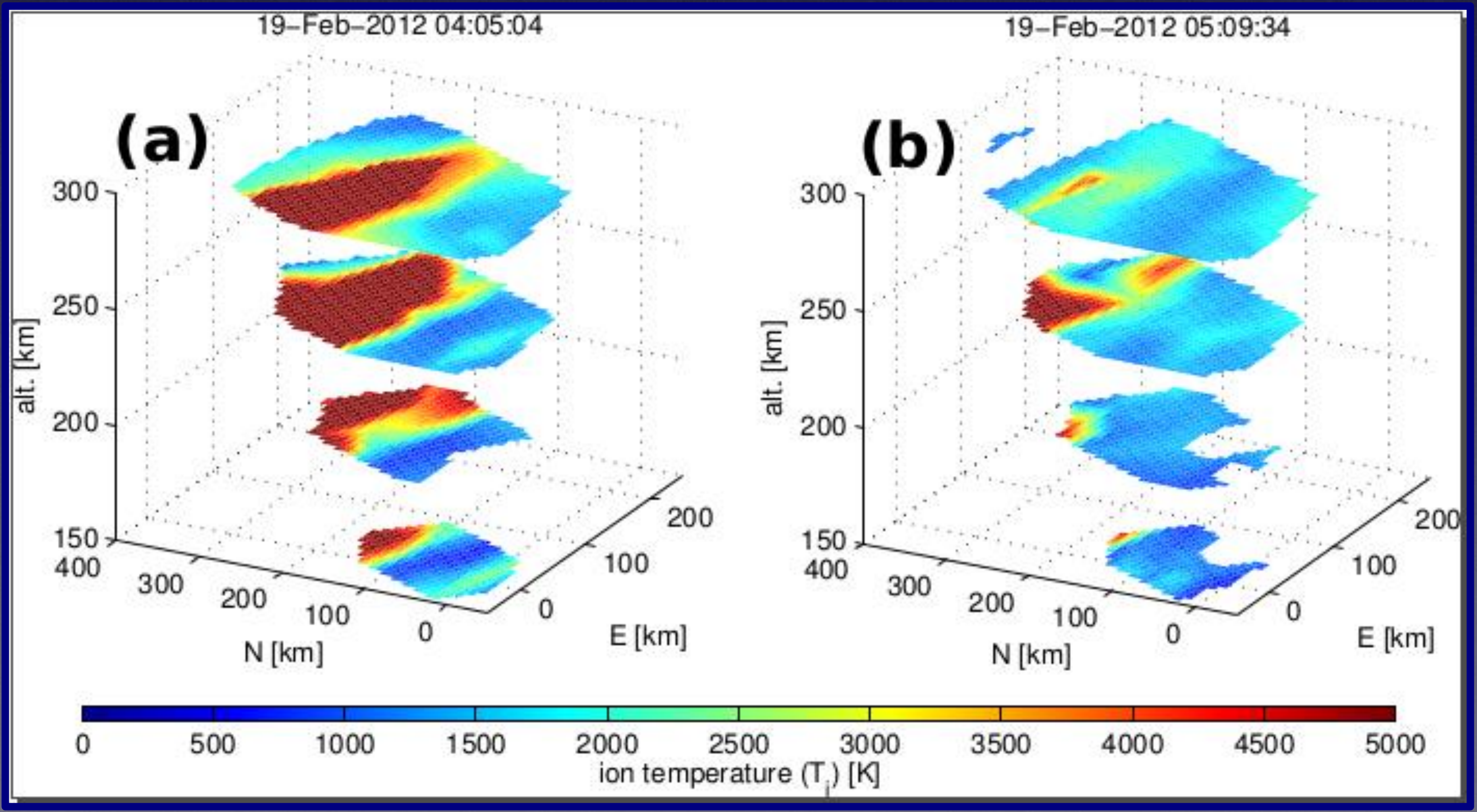

Zettergren, et al 2014

Moving beyond simple descriptions of upflow *drivers*

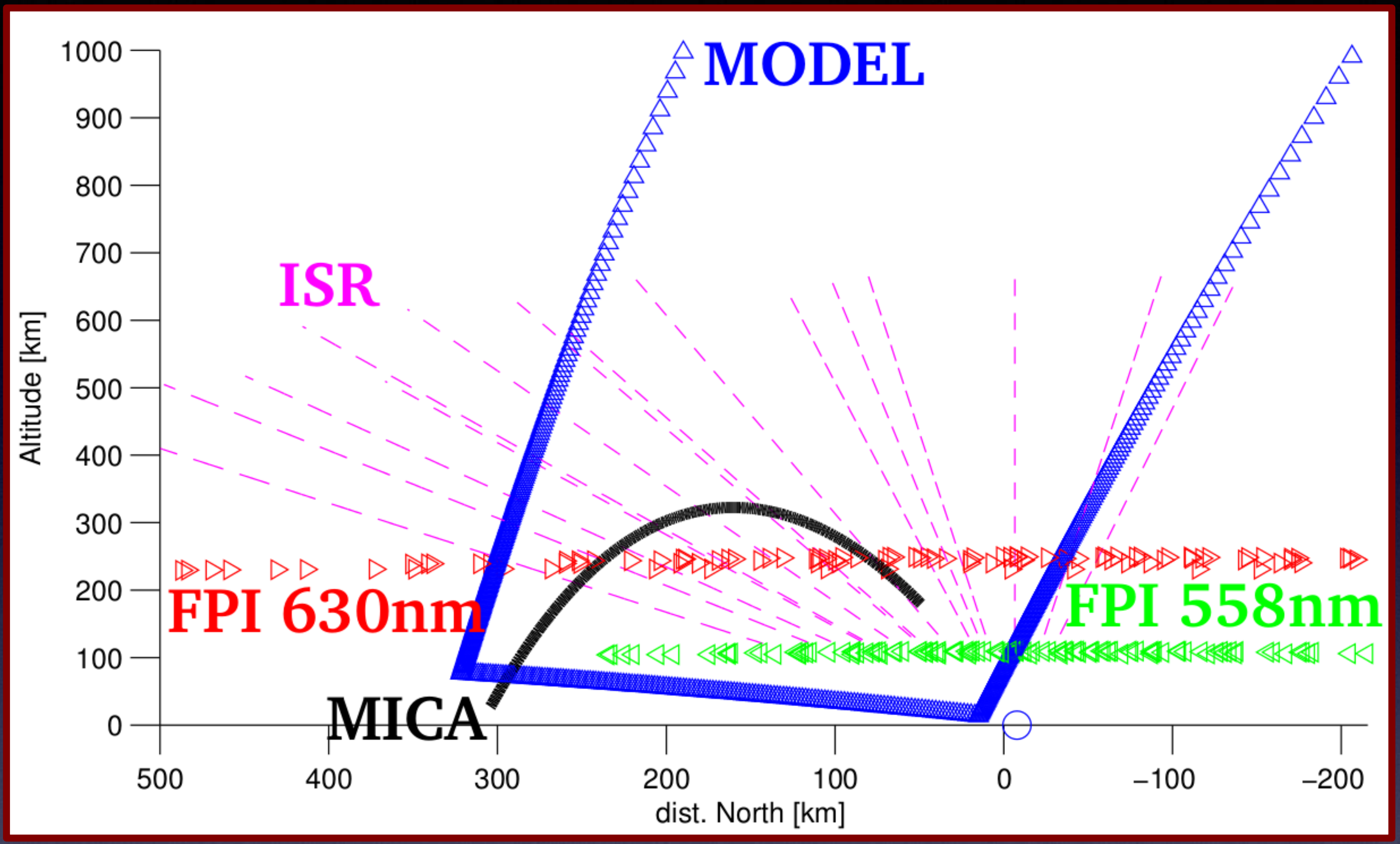

- ISR flows/fields via [Heinselman and Nicholls, 2008]
- SDI (FPI) winds [Conde et al]
- SDI + filtered allsky imager yields precipitation [D. Hampton]

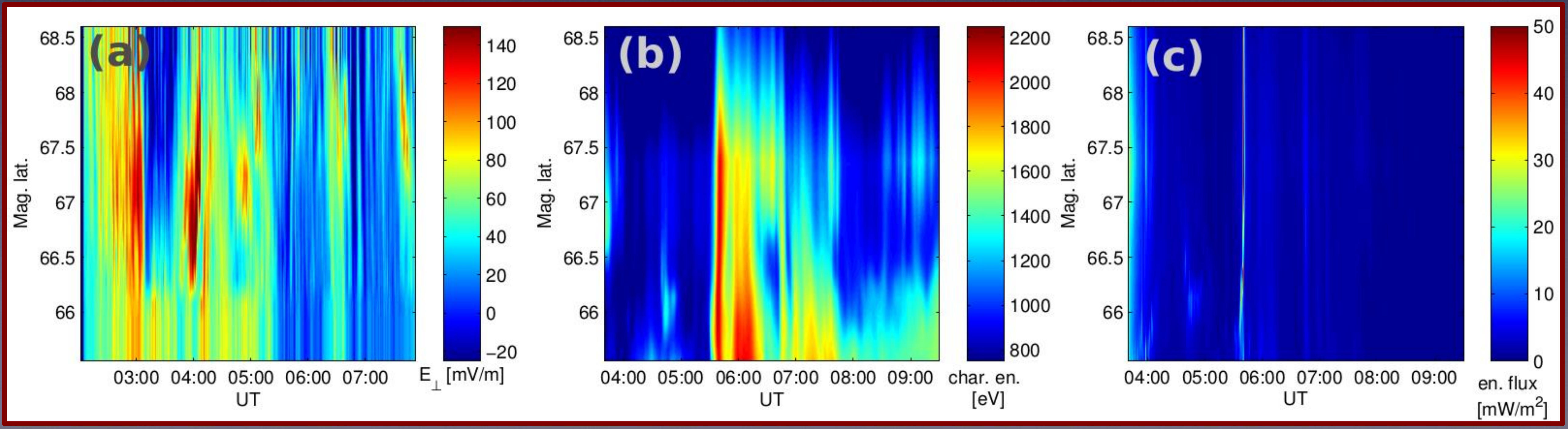

Modeled MICA density cavities

- Each DC electric field intensification associated with density depletion
- Depletions intermittently observed during ISR experiment
- Associated with growth phase and N-S streamer-related electric fields.

- ***Careful model decomposition shows these are due to molecular ion generation and enhanced recombination***

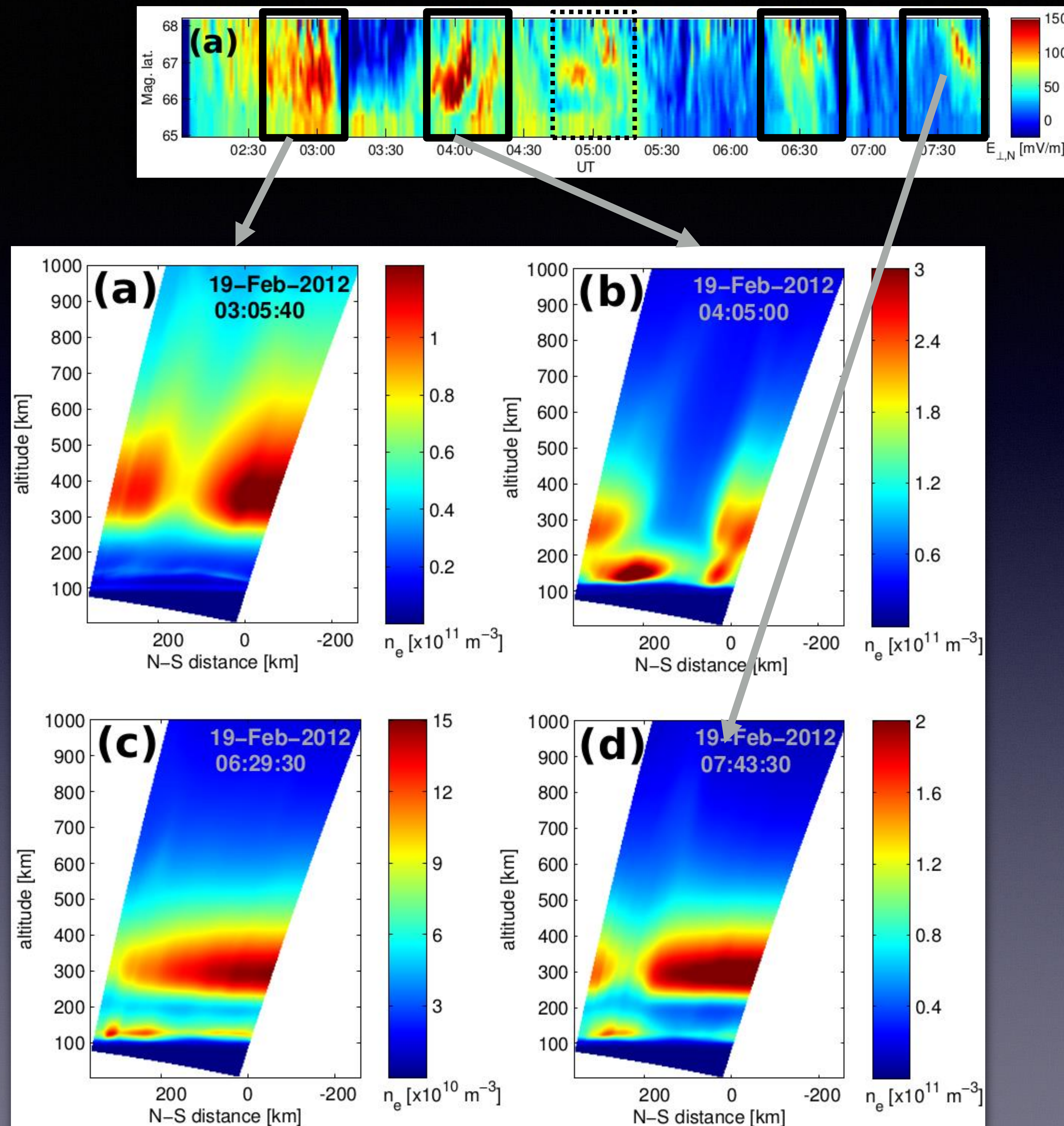

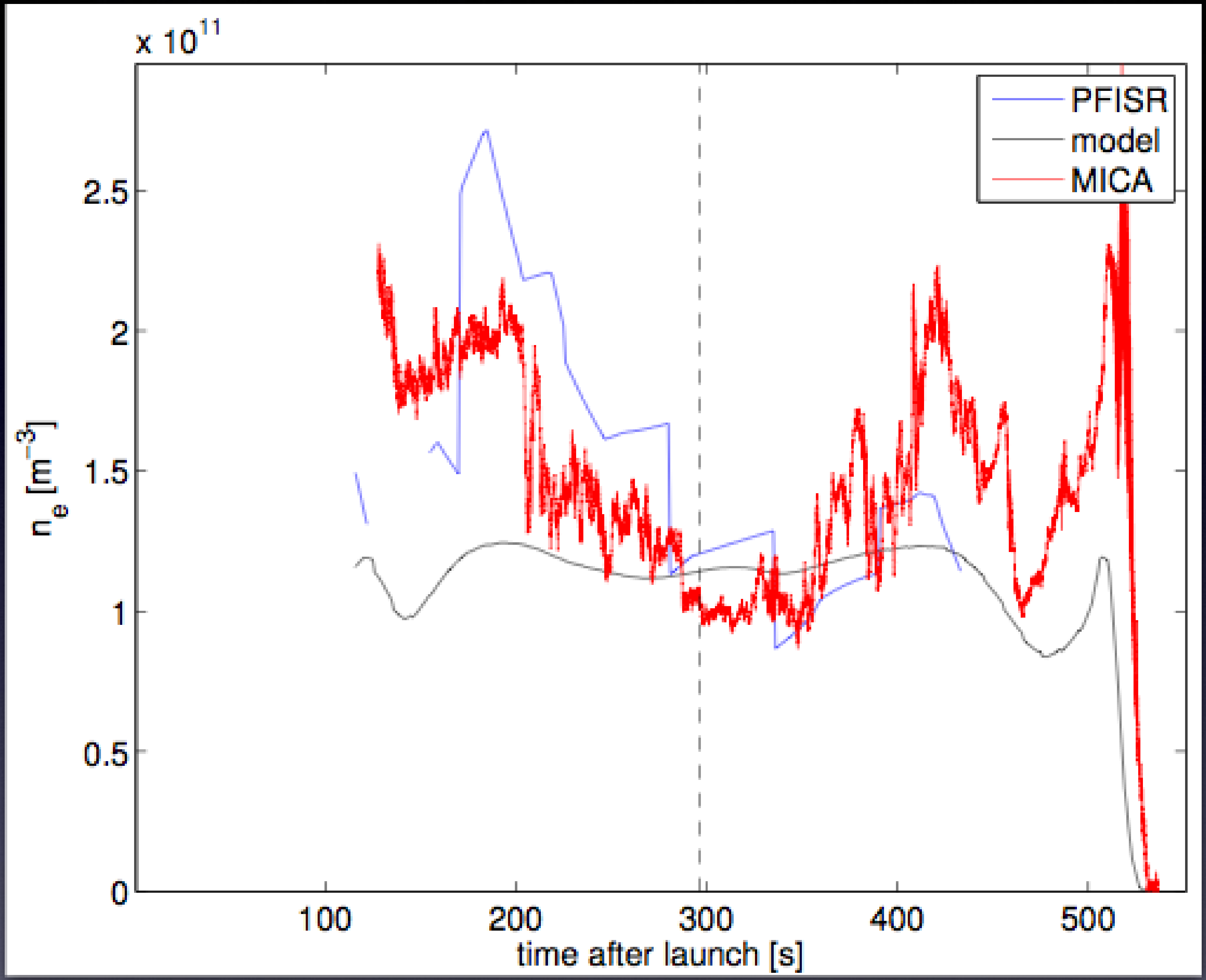

Density comparisons show basic consistency

MICA type-1 upflows

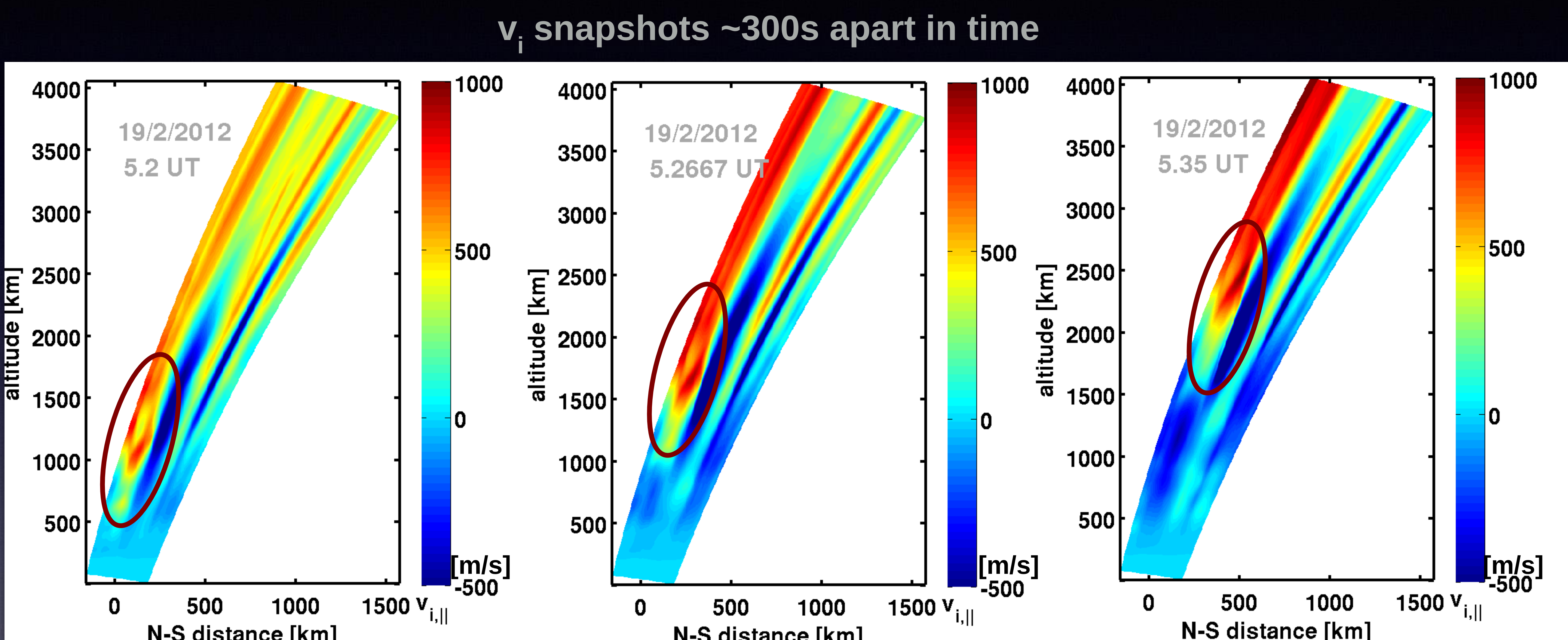

- Dynamic forcing can lead to upward transport of well-defined momentum features
- Overshoot and downflow are common in model results
- If downflow is intense enough it can cause compressional heating and secondary upflows
- These responses likely have an effect on seeding of ion outflow.

Fine-scale currents and flows

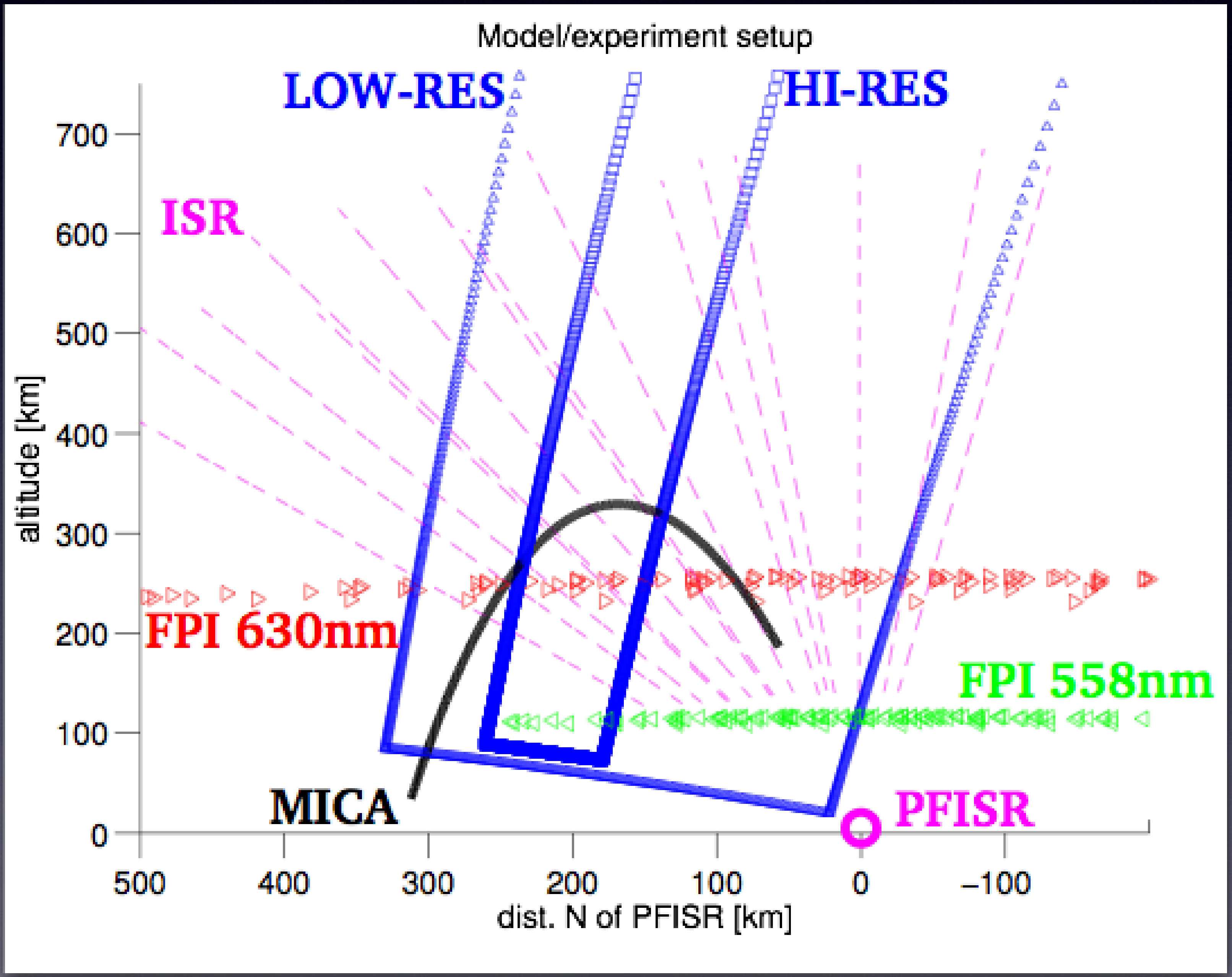

Lynch, et al 2015

Precipitation recovered by using a calibrated 427.8 nm narrow field imager at VEE (under apogee): triangulation + modeling gives characteristic energy and intensity gives total energy flux.

Modeled structure of “arc B”

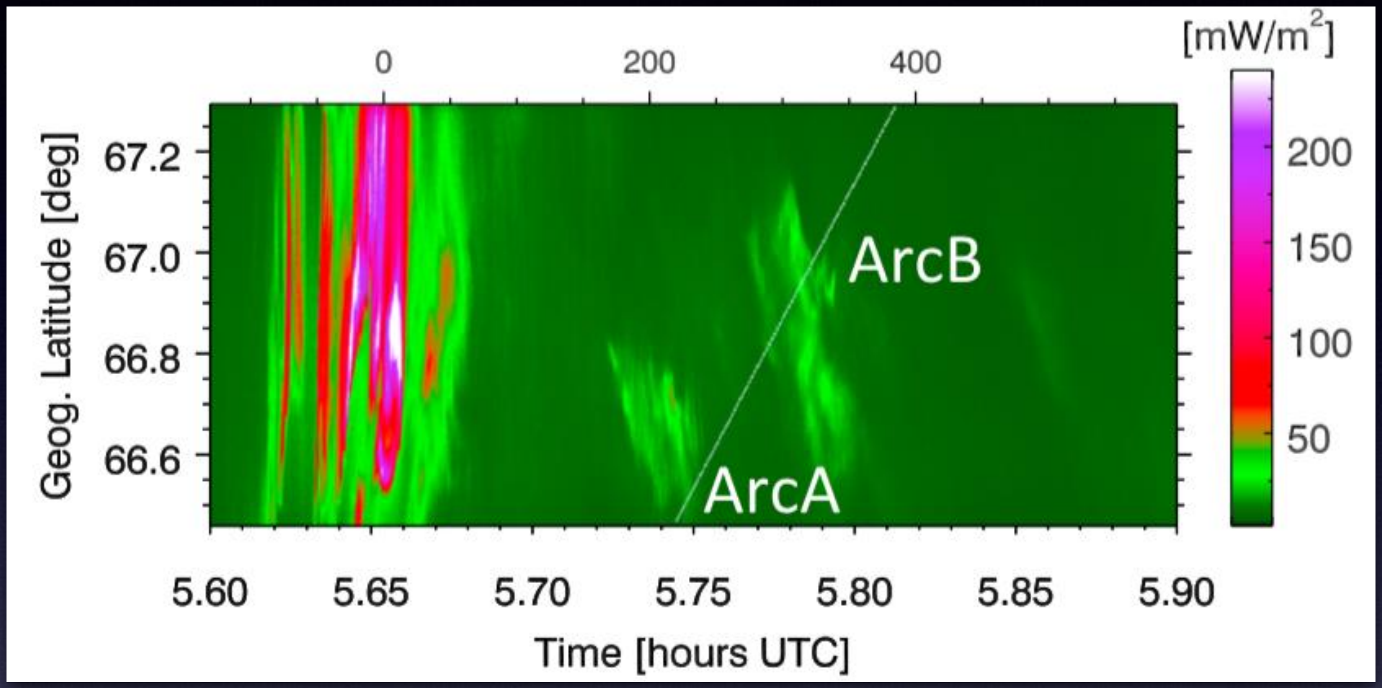

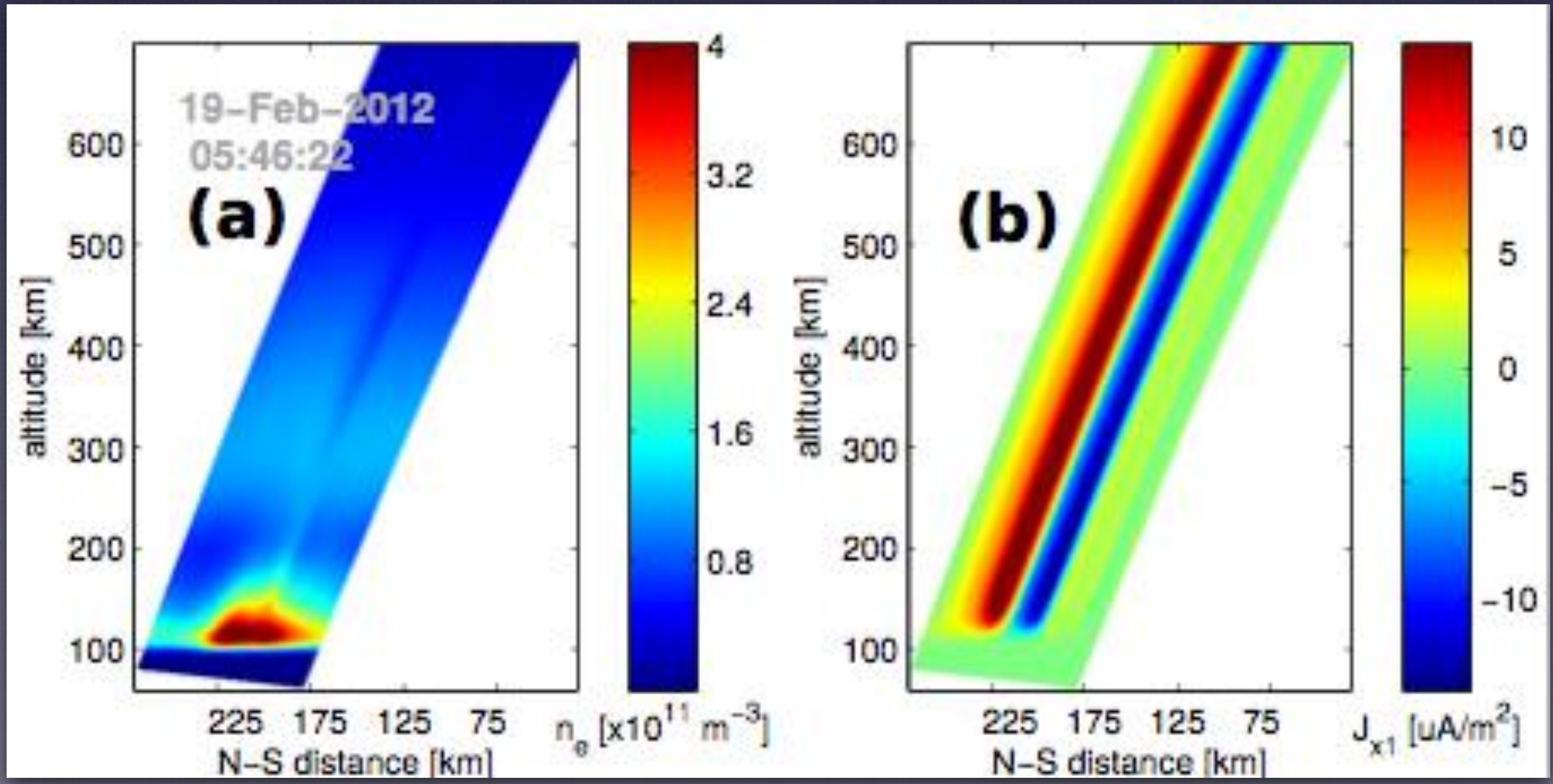

Fields and currents for fine-scale modeling

INPUT

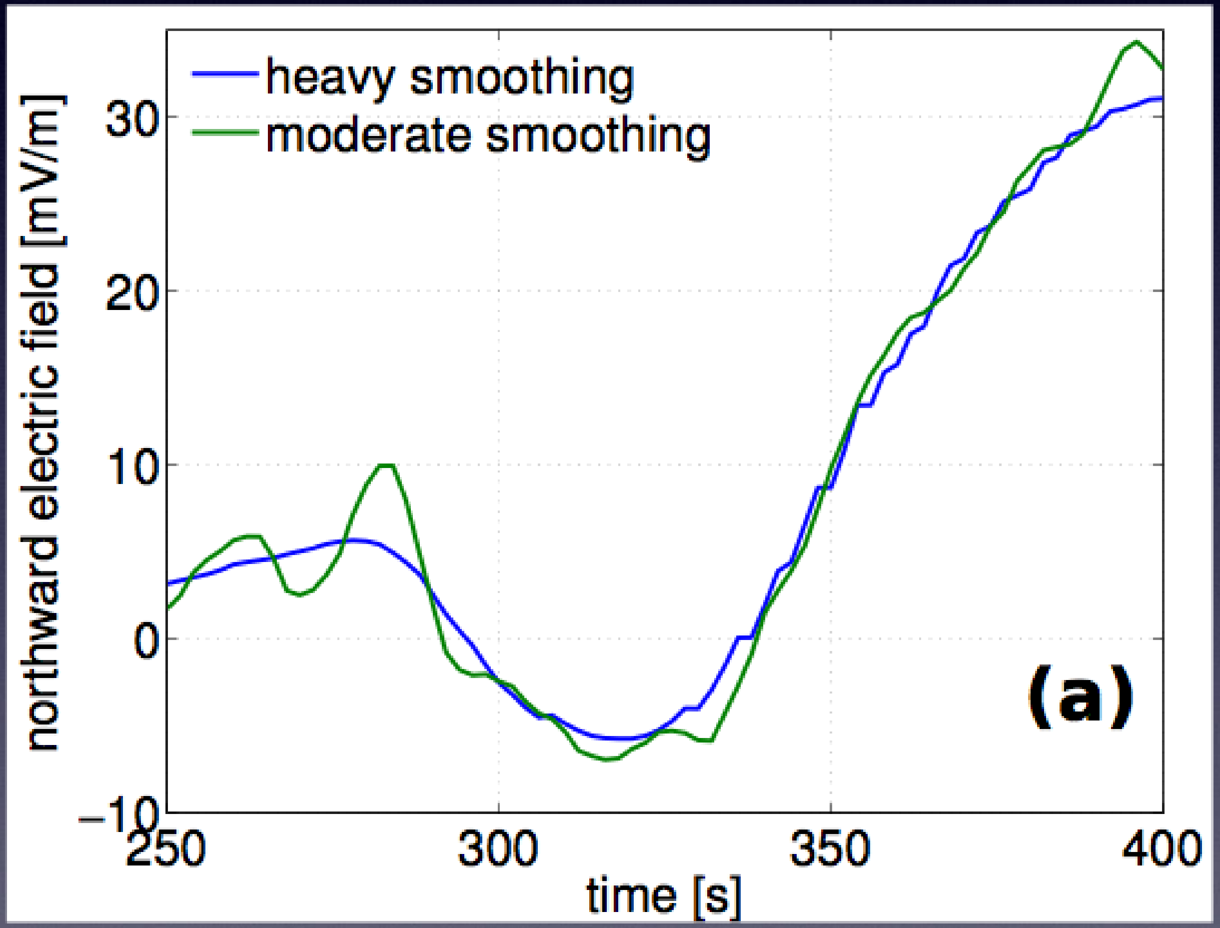

OUTPUT

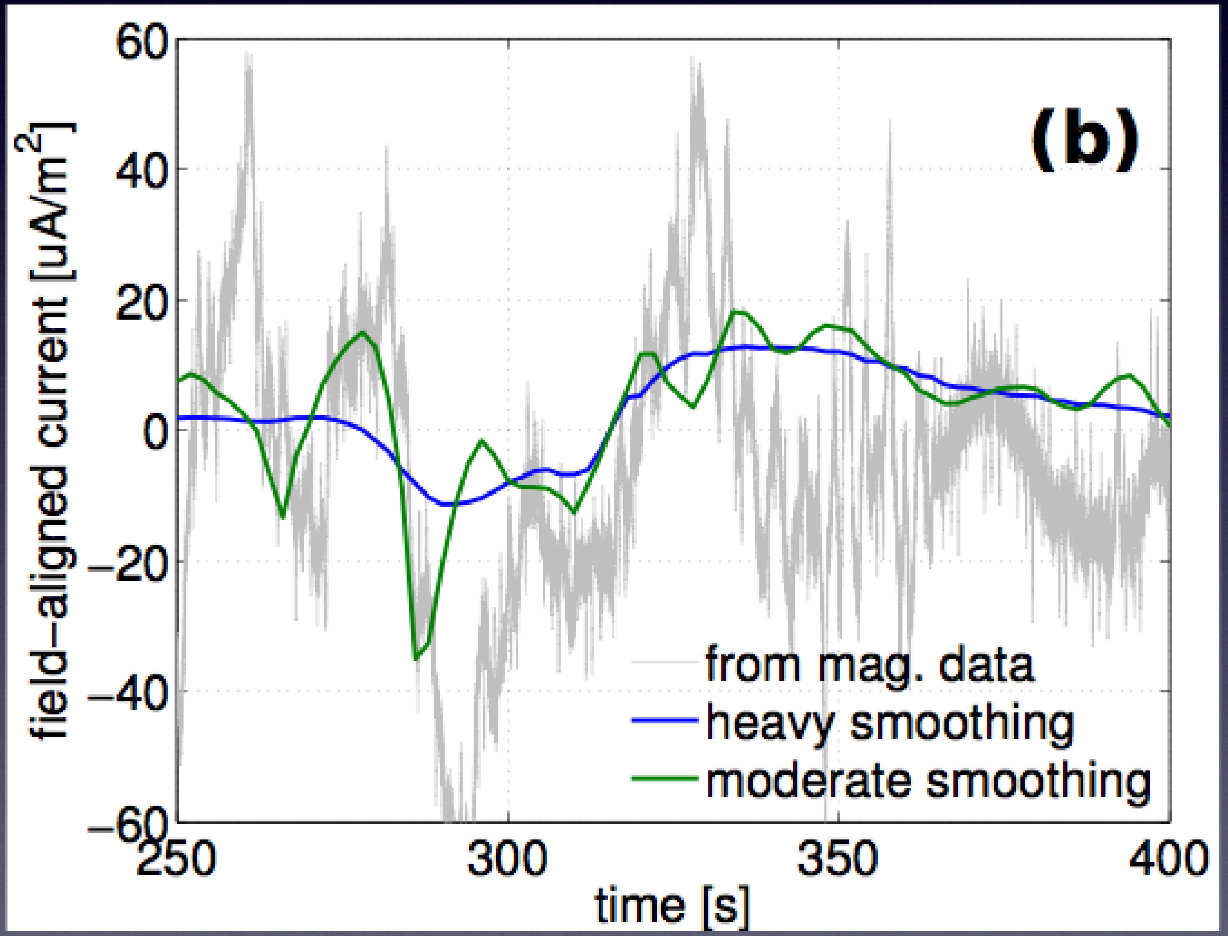

The model is able to mimc the basic electrostatic structure of the current systems

Contributions to total current density

Heavily smoothed simulation

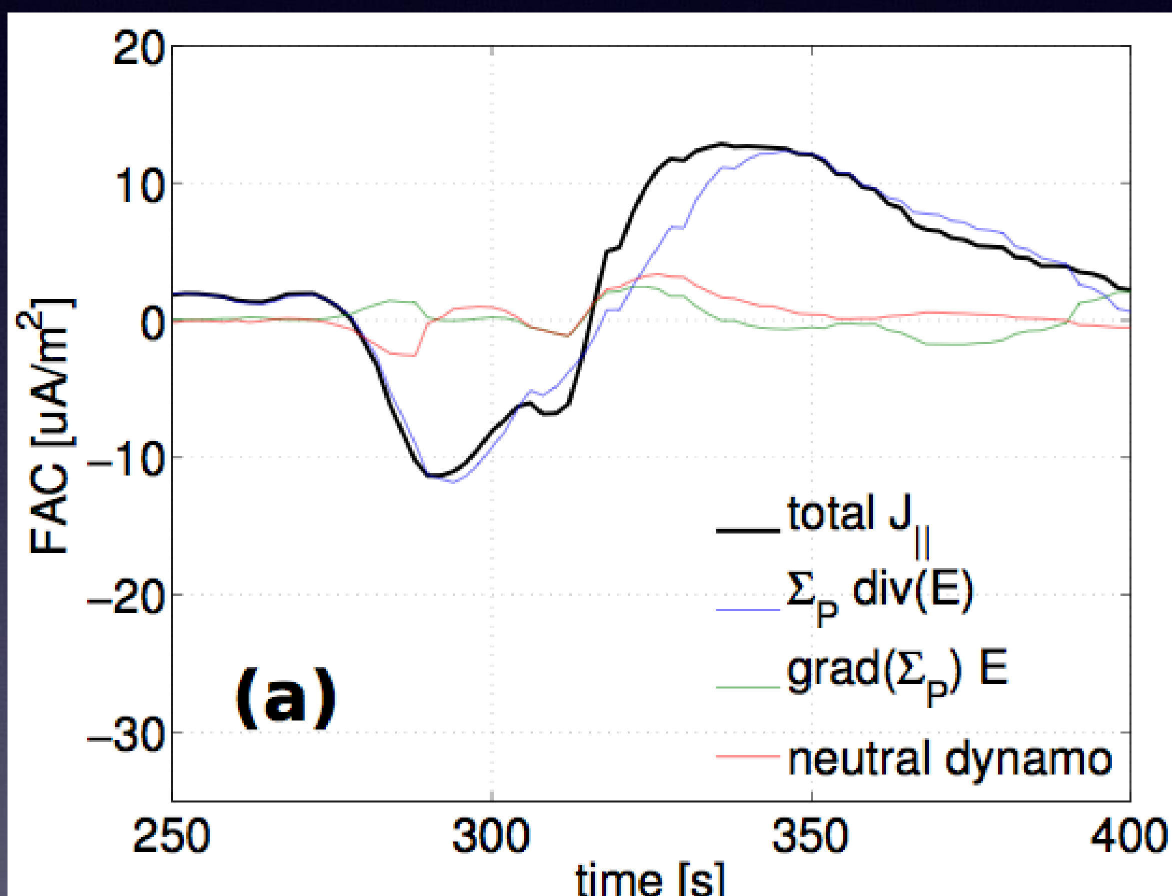

Moderately smoothed simulation

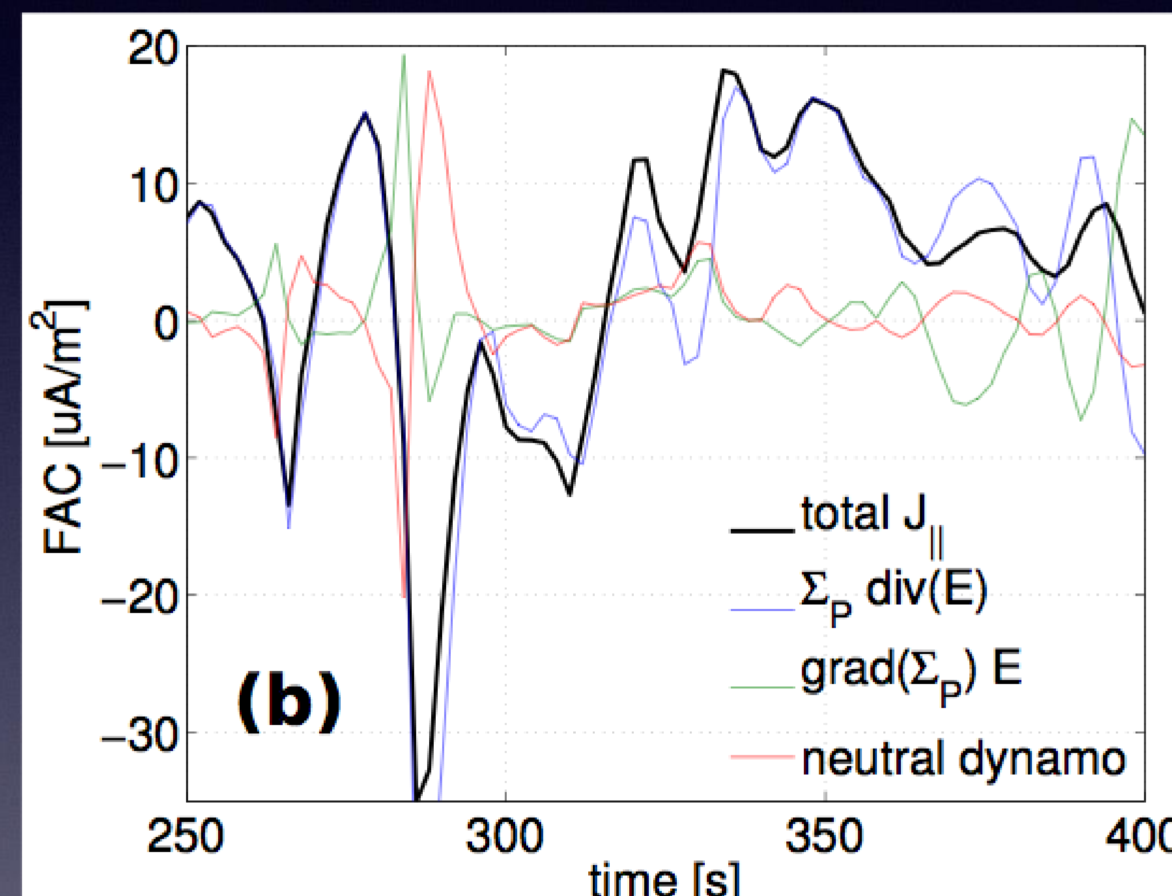

Electric field divergence dominates FAC, except near the up-to-down transition where conductivity gradients and winds contribute

Ion upflows

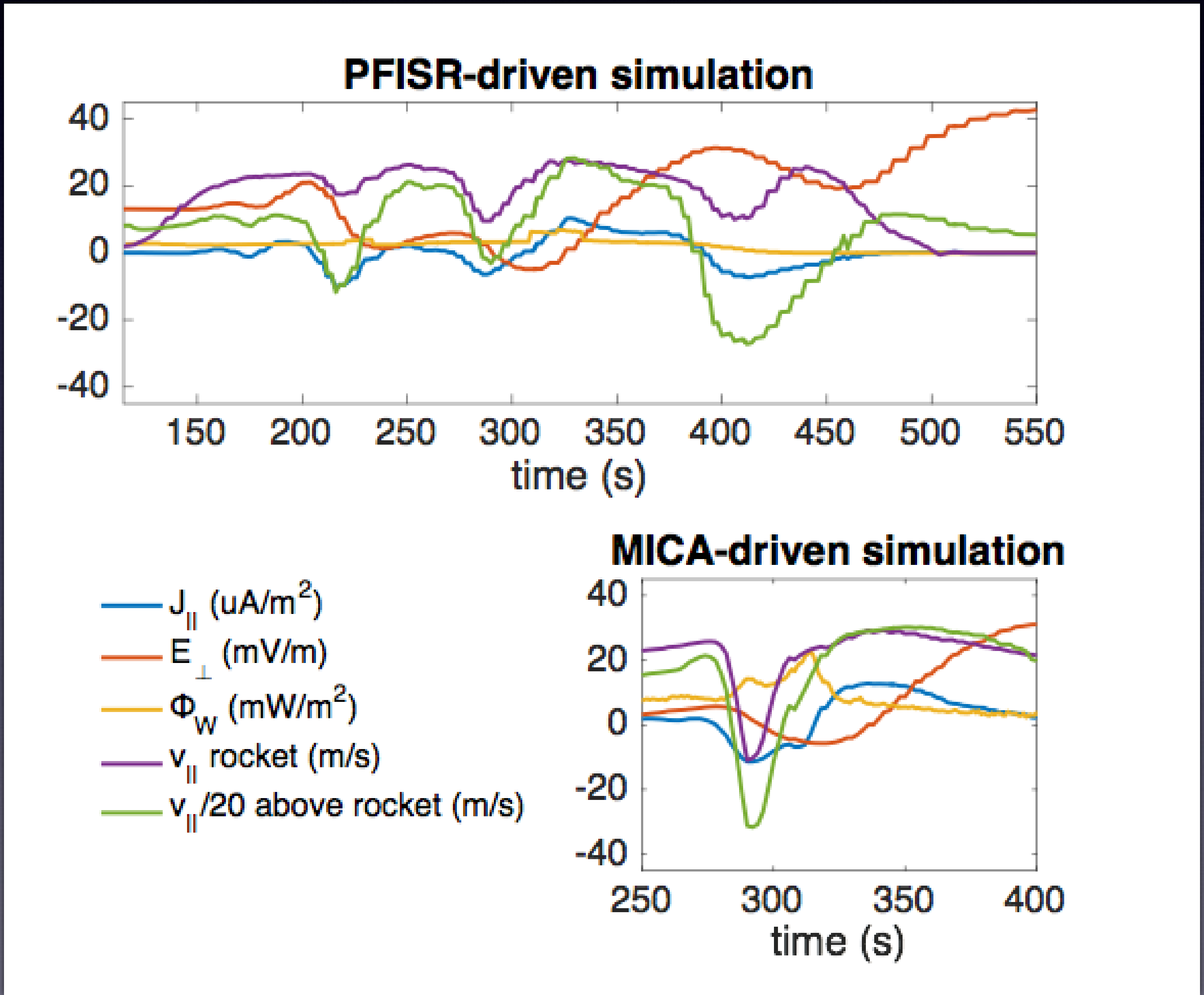

Large-scale modeling

Fine-scale modeling
(near apogee)

Fine-scale model (and data) shows upflow in UCR and downflow in DCR

Zettergren, et al 2014; Fernandes, et al 2016

Gemini-TIA

GEMINI-TIA model description:

$$\frac{\partial \rho_s}{\partial t} + \nabla \cdot (\rho_s \mathbf{u}_s) = m_s P_s - L_s \rho_s$$

$$\frac{\partial(\rho_s u_{s,\parallel})}{\partial t} + [\nabla \cdot (\rho_s \mathbf{u}_s \mathbf{u}_s)] \cdot \hat{\boldsymbol{e}}_\parallel$$
$$= \rho_s g_\parallel - \nabla_\parallel p_{s,\parallel} + n_s q_s E_\parallel - (p_{s,\parallel} - p_{s,\perp}) \nabla \cdot \hat{\boldsymbol{e}}_\parallel$$
$$+ \sum_j \frac{3 v_{sj}}{4\pi k_b} \left[2 k_b n_s m_s I_{002} \frac{\sigma_\perp}{\sigma_\parallel} (\mathbf{u}_t - \mathbf{u}_s)_\parallel + \frac{2}{\sigma_\parallel} (2 I_{202} - I_{002}) \left(\frac{n_s m_s h_{j,\perp}^\parallel}{n_j m_j} - h_{s,\perp}^\parallel \right) \right.$$
$$\left. + \frac{\sigma_\perp}{\sigma_\parallel^2} \left(\frac{2}{3} \frac{\sigma_\perp}{\sigma_\parallel} I_{004} - I_{002} \right) \left(\frac{n_s m_s h_{j,\parallel}^\parallel}{n_j m_j} - h_{s,\parallel}^\parallel \right) \right] + \sum_n n_s m_s v_{sn} (\mathbf{u}_n - \mathbf{u}_s)_\parallel$$

$$\frac{\partial p_{s,\parallel}}{\partial t} + \nabla \cdot (p_{s,\parallel} \mathbf{u}_s)$$
$$= -2 p_{s,\parallel} (\nabla_\parallel \cdot \mathbf{u}_s) - \nabla \cdot (h_{s,\parallel} \hat{\boldsymbol{e}}_\parallel) + 2 h_{s,\perp} (\nabla \cdot \hat{\boldsymbol{e}}_\parallel)$$
$$+ \sum_j \frac{3}{2\pi} \frac{\rho_s k_b v_{sj}}{m_s + m_j} \left[2 \frac{\sigma_\perp}{\sigma_\parallel} I_{002} (T_{j,\parallel} - T_{s,\parallel}) + m_j \left(\frac{2\pi}{3} (\mathbf{u}_s - \mathbf{u}_j)^2 + 2 \sigma_\perp (I_{200} - I_{002}) \right) \right]$$
$$+ \sum_n \frac{\rho_s v_{sn}}{m_s + m_n} \left[2 k_b (T_{n,\parallel} - T_{s,\parallel}) + 2 m_n (\mathbf{u}_s - \mathbf{u}_n)_\parallel^2 - \frac{m_n Q_2}{2 Q_1} \left(2 k_b (\sigma_\parallel - \sigma_\perp) - (\mathbf{u}_s - \mathbf{u}_n)^2 + 3 (\mathbf{u}_s - \mathbf{u}_n)_\parallel^2 \right) \right]$$

$$\frac{\partial p_{s,\perp}}{\partial t} + \nabla \cdot (p_{s,\perp} \mathbf{u}_s)$$
$$= - p_{s,\perp} (\nabla_\perp \cdot \mathbf{u}_s) - \nabla \cdot (h_{s,\perp} \hat{\boldsymbol{e}}_\parallel) + \dot{W}_{s,\perp} - h_{s,\perp} (\nabla \cdot \hat{\boldsymbol{e}}_\parallel)$$
$$+ \sum_j \frac{3}{4\pi} \frac{\rho_s k_b v_{sj}}{m_s + m_j} \left[4 I_{200} (T_{j,\perp} - T_{s,\perp}) + m_j \left(\frac{4\pi}{3} (\mathbf{u}_s - \mathbf{u}_j)^2 + 2 \sigma_\perp (I_{002} - I_{200}) \right) \right]$$
$$+ \sum_n \frac{\rho_s v_{sn}}{m_s + m_n} \left[2 k_b (T_{n,\perp} - T_{s,\perp}) + m_n (\mathbf{u}_s - \mathbf{u}_n)_\perp^2 - \frac{m_n Q_2}{4 Q_1} \left(2 k_b (\sigma_\perp - \sigma_\parallel) - 2 (\mathbf{u}_s - \mathbf{u}_n)^2 + 3 (\mathbf{u}_s - \mathbf{u}_n)_\perp^2 \right) \right]$$

Continuity Equation:

$$\frac{\partial \rho_s}{\partial t} + \nabla \cdot (\rho_s \mathbf{u}_s) = m_s P_s - L_s \rho_s$$

= (chemical production + photoionization + impact ionization) - (chemical loss processes)

Momentum Equation:

$$\frac{\partial(\rho_s u_{s,\parallel})}{\partial t} + [\nabla \cdot (\rho_s \mathbf{u}_s \mathbf{u}_s)] \cdot \hat{\boldsymbol{e}}_\parallel$$
$$= \rho_s g_\parallel - \nabla_\parallel p_{s,\parallel} + n_s q_s E_\parallel - (p_{s,\parallel} - p_{s,\perp}) \nabla \cdot \hat{\boldsymbol{e}}_\parallel$$
$$+ \sum_j \frac{3 v_{sj}}{4\pi k_b} \left[2 k_b n_s m_s I_{002} \frac{\sigma_\perp}{\sigma_\parallel} (\mathbf{u}_t - \mathbf{u}_s)_\parallel + \frac{2}{\sigma_\parallel} (2 I_{202} - I_{002}) \left(\frac{n_s m_s h^\parallel_{j,\perp}}{n_j m_j} - h^\parallel_{s,\perp} \right) \right.$$
$$\left. + \frac{\sigma_\perp}{\sigma_\parallel^2} \left(\frac{2}{3} \frac{\sigma_\perp}{\sigma_\parallel} I_{004} - I_{002} \right) \left(\frac{n_s m_s h^\parallel_{j,\parallel}}{n_j m_j} - h^\parallel_{s,\parallel} \right) \right] + \sum_n n_s m_s v_{sn} (\mathbf{u}_n - \mathbf{u}_s)_\parallel$$

= gravity – pressure gradient + ambipolar electric field – mirror force
+ ion-ion collisions [drag + perpendicular heat flow momentum transfer
+ parallel heat flow momentum transfer] + ion-neutral drag

Parallel Energy Equation:

$$
\begin{aligned}
\frac{\partial p_{s,\parallel}}{\partial t} &+ \nabla \cdot \left(p_{s,\parallel}\mathbf{u}_s\right) \\
&= -2p_{s,\parallel}(\nabla_\parallel \cdot \mathbf{u}_s) - \nabla \cdot \left(h_{s,\parallel}\hat{\boldsymbol{e}}_\parallel\right) + 2h_{s,\perp}(\nabla \cdot \hat{\boldsymbol{e}}_\parallel) \\
&+ \sum_j \frac{3}{2\pi}\frac{\rho_s k_b v_{sj}}{m_s + m_j}\left[2\frac{\sigma_\perp}{\sigma_\parallel} I_{002}\left(T_{j,\parallel} - T_{s,\parallel}\right) + m_j\left(\frac{2\pi}{3}\left(\mathbf{u}_s - \mathbf{u}_j\right)^2 + 2\sigma_\perp(I_{200} - I_{002})\right)\right] \\
&+ \sum_n \frac{\rho_s v_{sn}}{m_s + m_n}\left[2k_b\left(T_{n,\parallel} - T_{s,\parallel}\right) + 2m_n(\mathbf{u}_s - \mathbf{u}_n)_\parallel^2\right. \\
&\left. - \frac{m_n Q_2}{2Q_1}\left(2k_b(\sigma_\parallel - \sigma_\perp) - (\mathbf{u}_s - \mathbf{u}_n)^2 + 3(\mathbf{u}_s - \mathbf{u}_n)_\parallel^2\right)\right]
\end{aligned}
$$

= - compression – heat flux divergences + mirror effects
+ ion-ion collisions [heat exchange + frictional heating + par-perp heat transfer]
+ ion-neutral interactions [heat exchange + frictional heating
- par-perp heat transfer + additional frictional terms]

Perpendicular Energy Equation:

$$
\begin{aligned}
\frac{\partial p_{s,\perp}}{\partial t} &+ \nabla \cdot \left(p_{s,\perp} \mathbf{u}_s\right) \\
&= -p_{s,\perp}(\nabla_\perp \cdot \mathbf{u}_s) - \nabla \cdot \left(h_{s,\perp} \hat{\boldsymbol{e}}_\parallel\right) + \dot{W}_{s,\perp} - h_{s,\perp}(\nabla \cdot \hat{\boldsymbol{e}}_\parallel) \\
&+ \sum_j \frac{3}{4\pi} \frac{\rho_s k_b v_{sj}}{m_s + m_j} \left[4 I_{200}\left(T_{j,\perp} - T_{s,\perp}\right) + m_j \left(\frac{4\pi}{3} \left(\mathbf{u}_s - \mathbf{u}_j\right)^2 + 2\sigma_\perp (I_{002} - I_{200})\right)\right] \\
&+ \sum_n \frac{\rho_s v_{sn}}{m_s + m_n} \Bigg[2k_b\left(T_{n,\perp} - T_{s,\perp}\right) + m_n (\mathbf{u}_s - \mathbf{u}_n)_\perp^2 \\
&- \frac{m_n Q_2}{4 Q_1} \left(2k_b(\sigma_\perp - \sigma_\parallel) - 2(\mathbf{u}_s - \mathbf{u}_n)^2 + 3(\mathbf{u}_s - \mathbf{u}_n)_\perp^2\right)\Bigg]
\end{aligned}
$$

= - compression – heat flux divergence + mirror force
+ ion-ion collisions [heat transfer + frictional heating + par-perp heat transfer]
+ ion-neutral interactions [heat transfer + frictional heating
- par-perp heat transfer + more frictional heating]

$$
\dot{W}_i = 2m_i \left(\frac{\eta q_i^2}{4m_i^2}\right) |E_o|^2 \left(\frac{\omega_0}{\omega}\right)^\alpha
$$

Wave heating:
ω - local gyro-frequency for each ion
η - left-hand polarized fraction of the wave field
$|E_o|^2$ - wave power spectral density at reference frequency, ω_o
α - spectral power index

Sim #	Power Spectral Density (mV/m)^2/Hz	DC Electric Field (mV/m)
1	0	0
2	0.3	0
3	3.0	0
4	10.0	0
5	0	80
6	0.3	80
7	3.0	80
8	10.0	80
9	0	150
10	0.3	150
11	3.0	150
12	10.0	150

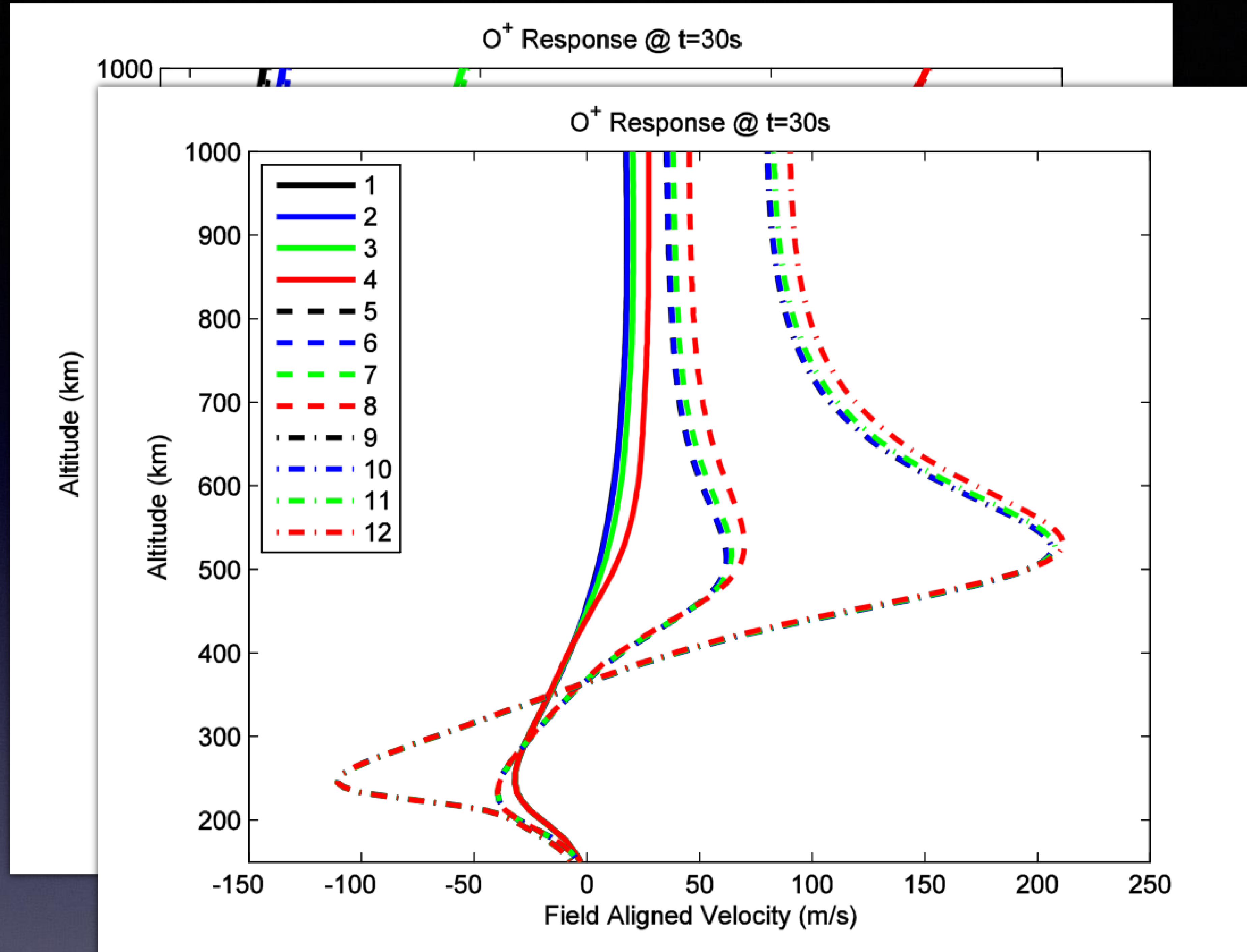

1) The DC electric field strength heavily influences the low altitude anisotropy and transverse wave heating dominates higher altitude responses
2) The stronger the PSD the deeper into the ionosphere a temperature anisotropy increased is observed

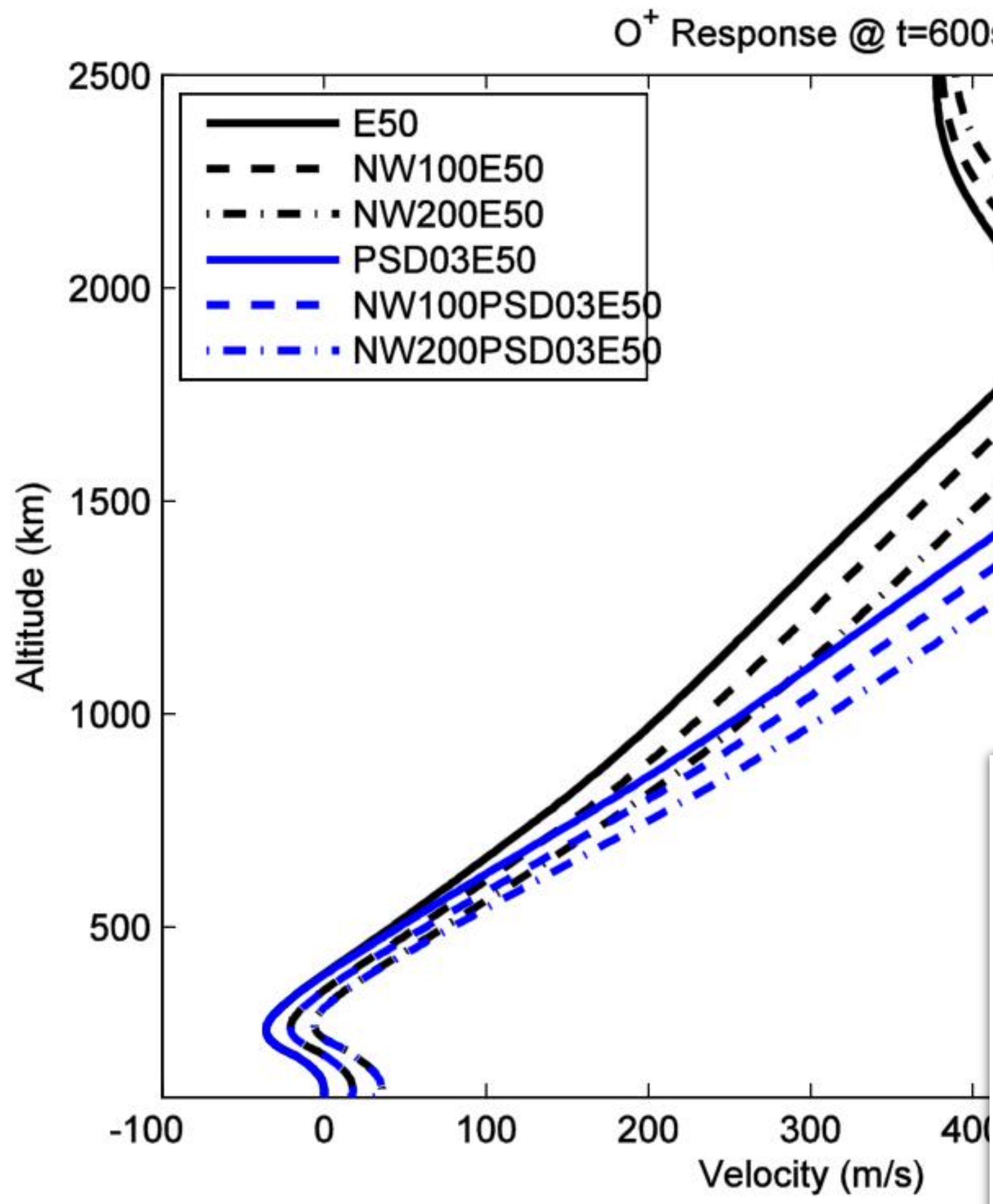

Neutral wind comments:

- A 200 m/s neutral wind is almost strong enough to overcome the negative flux from the pressure gradient at the f-region peak
- NW's can enhance upflows: the larger the NW the larger the ion velocity, even at high altitudes, if the wind is in a complimentary direction

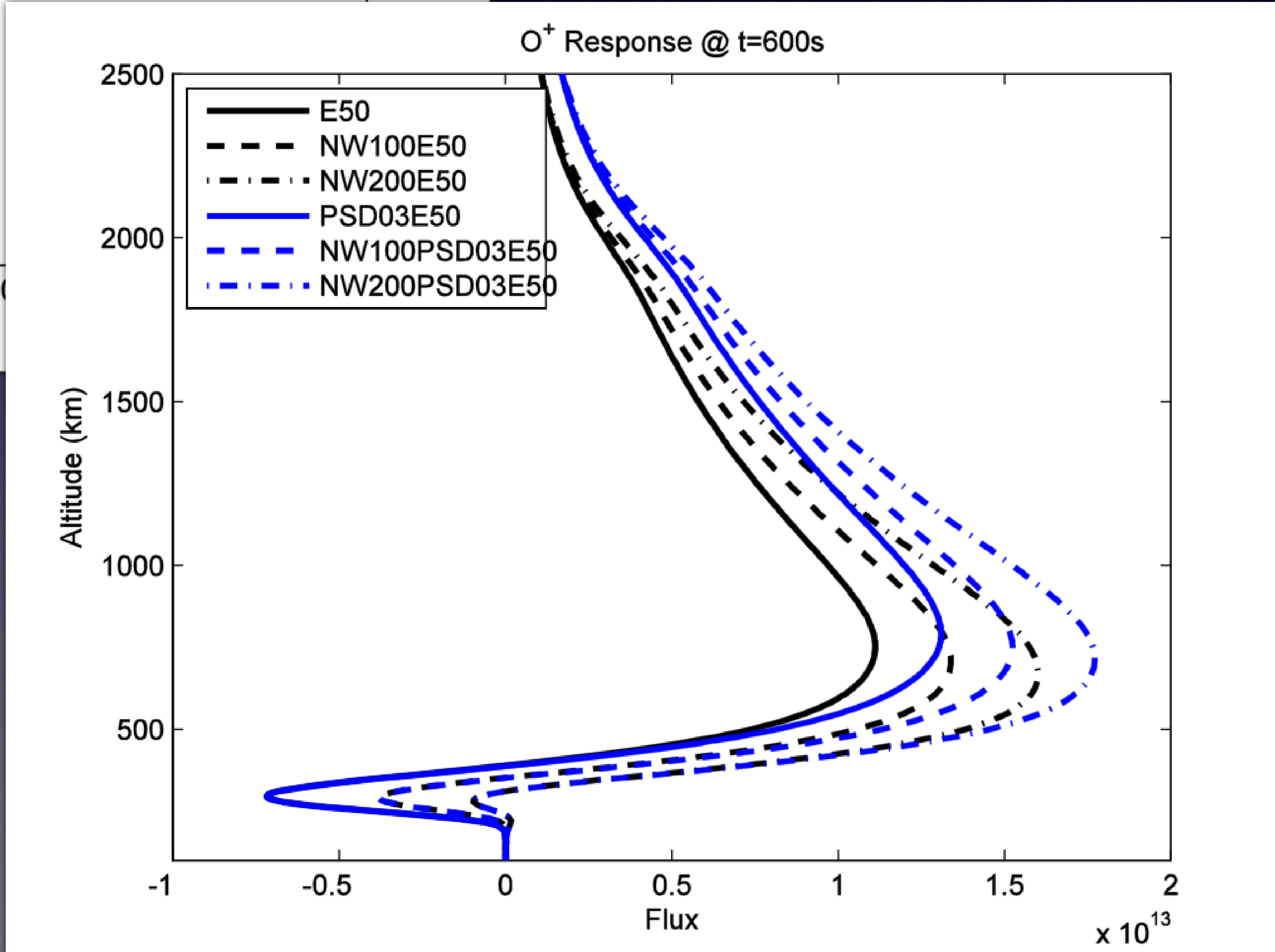

Wave heating comments:

- The reference PSD of 0.3 (mV/m)^2/Hz influences the ion response down to ~500km (this agrees with the literature)
- Wave heating can enhance the ion velocity by ~200m/s at 2000km
- Wave heating also increases the value and altitude of maximum ion flux